Proceedings of the ASME 2019 38th International Conference on Ocean, Offshore and Arctic Engineering
OMAE2019
June 9-14, 2019, Glasgow, Scotland

OMAE2019-95998

FEASIBILITY STUDY OF MOORING LINES DESIGN FOR A FLOATING TIDAL TURBINE PLATFORM USING DOUBLE HULL STRUCTURE

Nu Rhahida Arini[1], Philipp R. Thies, Lars Johanning
College of Engineering, Mathematic and Physical Science, University of Exeter
Penryn campus, Penryn, UK

Edward Ransley, Scott Brown, Nan Xie, Deborah Greaves
School of Engineering, Plymouth University
Plymouth, UK.
Rachel Nicholls-Lee, Whiskerstay Ltd, Falmouth, UK

ABSTRACT
This paper examines numerically the feasibility of a catenary mooring line for tidal energy platform. The platform is designed with two floating hulls and anchored by studlink chain on the seabed. The numerical model is validated against an experiment with 1:12 scale ratio. A mooring line tension positioned on starboard fore, platform surge and pitch motions are parameters to validate. The results show that the model agrees with experimental results. This paper also evaluates the feasibility of the mooring system when a tidal turbine is mounted and in operation. Two tidal turbine models are employed in the model. These are horizontal and vertical axis tidal turbines. Mooring performance analysis are investigated for both turbine conditions in a set of environmental condition. The result shows that mooring line using a vertical axis turbine experiences higher tension. For platform motions, the horizontal turbine generates slightly larger displacement in surge. However the pitch motion record shows equal displacement under both turbine operations.

Keywords: tidal turbine platform, double hull platform, platform mooring line, feasibility of mooring lines

NOMENCLATURE

f	fluid force
Δ	mass of fluid displaced by a body
a_f	fluid acceleration relative to earth
C_a	added mass coefficient for a body
a_T	fluid acceleration relative a body
ρ	density of water
v_T	fluid velocity relative to a body
C_d	drag coefficient for the body
A	drag area
$Ca\Delta$	constant related to the shape of the body and its displacement

1. INTRODUCTION
Tidal energy is one of the promising renewable energy resources to overcome the depletion of fossil fuel. Different from other renewable resources, tidal energy is predictable that is more reliable to harness. However the tidal turbine system so far has not been established yet. In general tidal energy system is constructed from a floating platform where a tidal turbine is mounted. The platform is moored on the seabed by means of chain lines or ropes. The mooring lines maintain the platform at its designed position. The lines should also be adaptable with the environmental loading such as loads from wave, current and wind at the site. Therefore the mooring system requires a careful design so that it is able to hold platform from the turbine thrust as well as forces from the environmental condition.

The mooring system is a high cost in an offshore renewable energy system's expenditure. The installation cost contributes 20% to total cost of tidal renewable energy device [14]. A good mooring line system can also reduce installation cost by 30-40% [14]. Therefore the mooring system design is crucial. This paper aims to study the feasibility of a mooring system design for a tidal energy platform. The feasibility study will be performed numerically by developing a hydrodynamic model and validated against experiment which is conducted in a flume tank with 1:12 scale ratio.

In tidal energy system construction, a mooring system is developed to achieve the platform station keeping from the offshore fluid loading. [9] discussed a mooring system for the use of offshore renewable energy converter. He stated that a catenary mooring system is highly recommended for renewable

[1] Contact author: n.arini@exeter.ac.uk

energy converter in shallow or intermediate deep water. The use of catenary lines is beneficial such as minimize force working at the anchor while simplify the restoring force. The restoring force in the catenary mooring comes from the weight of the lines which maintains the platform at a secure position with certain permitted tolerance. Researchers have developed mooring line models and validated with experiments such as discussed by [2, 12]. They developed a new code for mooring dynamic analysis and found that the codes can predict the dynamic behavior of mooring lines satisfactorily.

In this paper the hydrodynamic mooring system model is developed in OrcaFlex 10.2. The model consists of double hull floating platform which is moored by four lines and anchored to the seabed. A set of environmental condition is demonstrated in the model to define sea depth, current velocity, wave height and period. It is assumed that there is no current variation in vertical direction. A set of environmental condition is shown in Table 1.

TABLE 1: ENVIRONMENTAL CONDITION

depth (m)	12
Current velocity (m/s)	1.75
Reg. wave frequency (Hz)	0.51
Wave height (m)	0.5-1.25
Wave period (s)	6.5-7

The platform is designed using double hull floating structure which is manufactured from two cylindrical pipes. The hulls are connected by the square frame where the turbine is mounted. The technical drawing of the platform is shown in Figure 1.

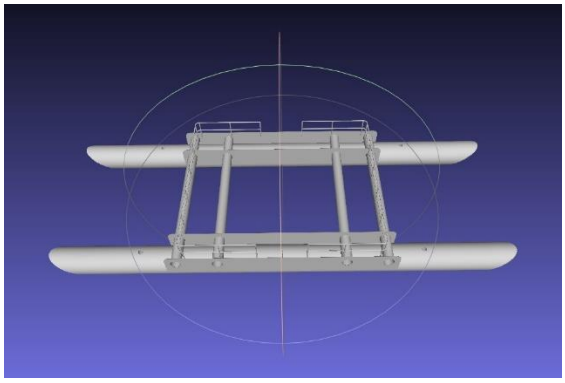

FIGURE 1: DOUBLE HULL FLOATING PLATFORM

The feasibility study is performed by generating a mooring system model and validate the model results against experiment. A line located in starboard fore will be validated. The tension of the line, platform motion in surge and pitch from the model are compared with the experiment. The validated model is further used to examine the mooring system when a turbine is attached and in operation. Horizontal and vertical axis tidal turbines are employed and modelled separately. Mooring performance analysis of the mooring lines under each turbine's operation are performed. All of the concept of model and experiment will be detailed in Section 2. The validation result and performance analysis will be highlighted in Sections 3 and 4 respectively.

2. HYDRODYNAMIC MODEL

A hydrodynamic model of mooring system for tidal energy platform is discussed in this section. The mooring lines utilize catenary configurations with the properties written in Table 2. The floating platform is constructed from double hull pipe with the geometry is also written in Table 2.

TABLE 2. MOORING LINE AND PLATFORM GEOMETRY IN FULL SCALE

	Mooring lines	Platform
Type	Studlink chain	Double hull
Bar diameter	50 cm	0.45 m
Length	130 m	20 m
Mass	0.537 kN/m	20 te

The model is developed from a floating platform which is moored on seabed with four catenary lines with 30^o spread from longitudinal axis. All the mooring lines are manufactured from steel studlink chains with properties as shown in Table 2.

Mooring lines are long and slender structures which is assumed only axial force acting on it. The lumped mass method is widely used to analyze the mooring system including OrcaFlex 10.2 [10]. The loading experienced by a line is obtained from Morison's equation, as written in equation 1, which consists of all hydrodynamic (wave and current) and aerodynamic (wind) forces.

$$f = \left(\Delta a_f + C_a \Delta a_T\right) + \frac{1}{2}\rho C_d A v_T |v_T| \qquad 1$$

The analysis is performed in static and dynamic calculation. The static analysis has been discussed by [4]. In the analysis the line is treated as a static system by neglecting any external forces hence no motion is considered. It is a global analysis and the likely result is in the form of general outcomes such as total force. Researchers have also analyzed dynamic mooring system intensively [8, 12]. The external forces coming from wave, current and wind are considered. The forces generate mooring system motion as the response of interaction between mooring system and the loading. The interaction is modelled by a vibration system as detailed by [1, 2]. The line is discretized. The fluid loading generates an axial motion which change the contact length with the seabed. This generates unsteady upward motion at all points along the lines.

Parametric study of catenary mooring dynamic response has been discussed by [8]. In their analysis the dynamic response was results of the interaction with the platform and environment. They found that increasing mooring stretch can reduce platform motions. In this paper the mooring line is discretized into target

segments and its motions are modelled by vibration with spring and damper system. The mooring line is modelled as a line pipe in OrcaFlex as depicted in Figure 2 and the mooring line configuration model in OrcaFlex is shown in Figure 3.

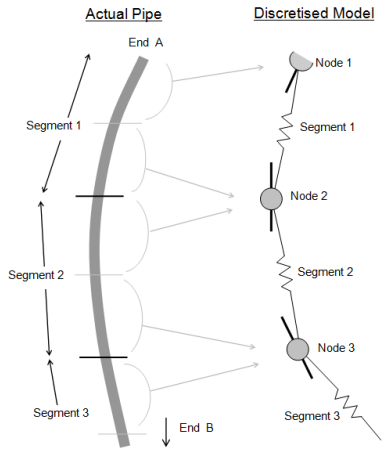

FIGURE 2: LUMPED MASS FOR LINE MODEL [10]

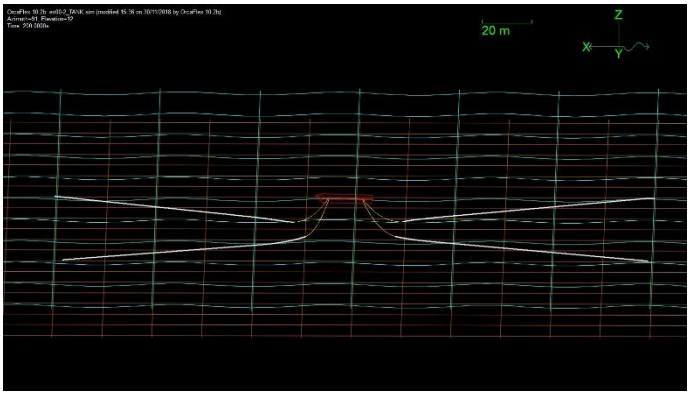

FIGURE 3: ELEVATION VIEW OF MOORING LINE SYSTEM LAYOUT

For the validation case, the wave is modelled in regular form using Stokes' 5th [5] mode. Further in the validated model, irregular wave from JONSWAP mode will be employed to examine the mooring performance of the model with a tidal turbine attached. The mooring performance analysis is a preliminary assessment to identify rigorous fatigue and failure damage of the mooring system.

In validation case the current and the wave propagate from the same directions as also indicated by the arrow direction on the axis line in Figure 3. The wave and current transmitted toward the rear of the platform. The lines in Figure 3 from top left clockwise is denoted as line 1, 2, 3 and 4. The regarded lines are positioned at starboard fore, starboard aft, port aft and port fore respectively. The validation is performed comparing model result of line 1 tension, platform surge and platform pitch motions to the experiment.

The catenary mooring line is modelled by pipe line type in OrcaFlex with target segments of 0.3 m length. The end connection type is fixed at seabed and assumed without torsional force. Stiffness of all mooring lines at both ends are neglected. The platform is modelled by a vessel type. Hydrostatic stiffness, frequency dependent added mass and damping and load RAO (Response Amplitude Operator) are designed for platform six degree of freedom motions. The added mass and damping have 20 frequencies. Load RAO is defined in 8 angles from 0 until 360 degree with the gap of 45 degree. Centre of gravity is located at the centre of platform.

In this paper the model is performed with preliminary static analysis prior to dynamic simulation. For dynamic calculation, the model is run for 200 seconds with 0.01 second time step. Each time step has 100 maximum number of iterations using $25x10^{-6}$ tolerance. In the static simulation, the model is set with 7300 max iterations using 10^{-6} tolerance.

The model is designed with two types of platform RAO. RAO determines the response motion of floating structure under a dynamic fluid loading using statistically approach. The RAO used in the model are displacement RAO and wave load RAO. Displacement RAO defines the first order motion of the platform in response to waves of given period and amplitude. The load RAO defines the first order wave force and moment on the platform due to waves of given period and amplitude [10]. Another important parameter for hydrodynamic model is hydrostatic stiffness. This determines displacements and deformations of a platform under dynamic fluid loadings. The stiffness represents the oscillations response of the platform since it is modelled as a vibration mode. It is a complex parameter for a floating structure. [15, 16] discussed how to obtain numerically the stiffness for marine structures. In the model hydrostatic stiffness is performed in six degree of freedom platform motion.

3. EXPERIMENT

An experiment was conducted to validate the mooring system model discussed in Section 2. The experiment was carried out at the Ocean Basin of the COAST Laboratory of University of Plymouth. The experiment set up is shown Figure 4. Length and width of the basin are 35 m and 15.5 m respectively. The basin has a movable floor and the water depth for the experiments was 1 m. Waves were generated by 24 individually controlled hinged flap absorbing paddles. A convex absorbing beach was installed at the opposite end of the basin. The current was generated by a recirculating system [13].

The experimental model was manufactured with scale ratio of 1:12. The geometry of the underwater part of the model is similar to that of the full scale device. The above waterline part including deck layout were simplified. The hulls (two cylinders) were made of plastic tubes and the supporting frames are of aluminum tubes. The cross beams and the ballast weight inside the hulls were selected such that the mass, CoG position and radii of gyration of the model were scaled from the full scale device.

The model motions were measured by an optical tracking system. Waves and current velocities were measured by using

resistance type wave probes and current flow meters, respectively. A 6-aixs load cell was used to measure fluid loadings on the model hull when it was fixed. The capacities of the load cell are 125 N for Fx and Fy, and 250 N for Fz. Capacity of Mx, My and Mz are all 25 N.m. Accuracy of the load cell is ±0.1%.

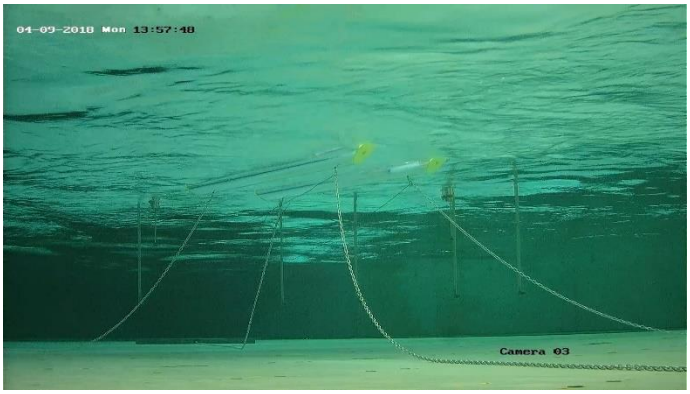

FIGURE 4: EXPERIMENTAL SET UP

Four catenary mooring lines were used for the platform in its floating condition, with two at the bow and another two attached at the stern of the twin hull. The angle of spreading mooring lines with *x*-axis (longitudinal direction) was 30 degrees. The weight of the mooring line chain in water is 37.7 kg/m and the water depth is 12 m in full scale. The chain used for the mooring lines in the experiments is 4 mm galvanized short link chain.

The experiments are performed with two current conditions. First experiment is performed without applied current and the second is with 0.167 m current speed.

4. RESULT AND DISCUSSION

Line 1 tension, platform surge and pitch motions from model is recorded for 200 seconds and compared to the experiment. Two set of environmental conditions are simulated and tested for validation purposes. First case is modelled with no current applied and the second is run with 0.579 m/s current speed.

4.1. VALIDATION

The comparison of the model and experimental results for mooring line tension in the case with no current and with 0.579 m/s current are shown in Figure 5 and 6 respectively. Both cases are run for 200 seconds. At the initial period, the model and experiment experience instability which is indicated by the irregular signal at first 50 seconds approximately. After that the signals period are found to be regular which is produced by a regular wave employed in this case. The wave forms a sinusoidal signal and generates sinusoidal line tension. The line tension fluctuation is at high peaks when the wave approaches and hits the mooring line. The wave pulls the line away from its equilibrium position such that produce higher tension on the line.

From Figure 5 it can also be seen that mooring line tension frequency agrees with the experiment. The signal amplitude is found to be 4.8 kN. Both experiment and model signal coincides at the same mid line which is roughly 9.2 kN. This indicates that both signals have the same average value. The second validation case is performed with current applied in the model. The line 1 tensions from model and experiment are shown in Figure 6.

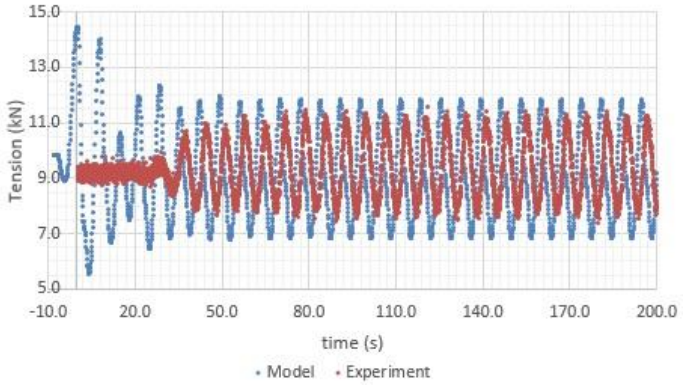

FIGURE 5: VALIDATION OF MOORING TENSION IN CASE WITH NO CURRENT

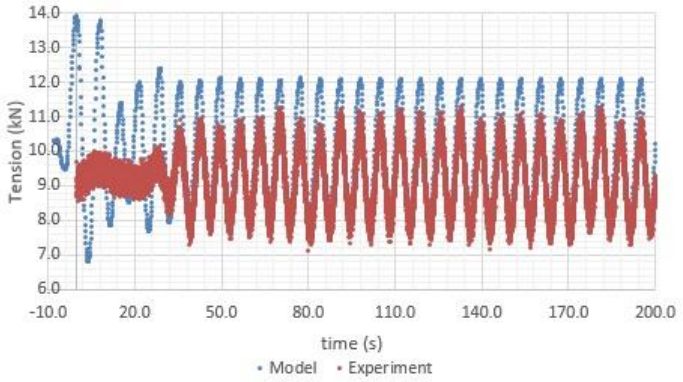

FIGURE 6: VALIDATION OF MOORING TENSION IN THE CASE WITH CURRENT

The model and experiment results for the case with current shows have equal frequencies and signal amplitude. However the model slightly over predict the tension magnitude such that the average tension is higher than the one from experiment. This demonstrates that the fluid loading experienced by the model is higher than the experiment although the loading has the same range. This is likely due to the wave model selected in the model in which does not produce appropriate wave and current loading as in the experiment accordingly.

Comparing to the model with no current in Figure 5, the tension experienced by line 1 in the case with current is higher. This indicates that fluid loading acting on the line is stronger. The more element constructing/forming the fluid loading generates higher tension. Thus it is more reliable to also take into account the effect of other loads for instance wind load, so that the condition is close to environment when modelling a mooring system. In both cases, wind effect is neglected.

The second stage validation is to compare the platform motion for both models, with and no current applied. The

displacement in surge and pitch directions in the case with no current from model and experiment are shown in Figures 7 and 8 respectively.

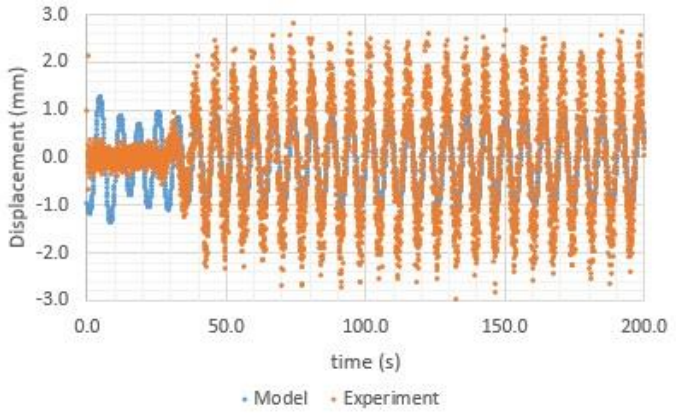

FIGURE 7: VALIDATION OF PLATFORM SURGE IN THE MODEL WITH NO CURRENT

Figure 7 shows that frequency and average of platform surge motion agree with the experiment. However the model displacement are less than one from experiment. This trend does not happen in the pitch motion as shown in Figure 8 below.

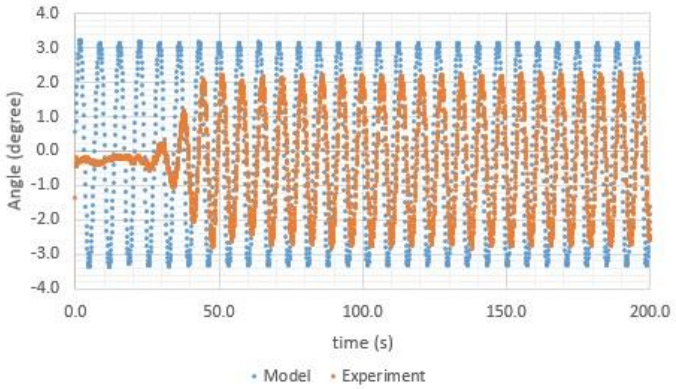

FIGURE 8: VALIDATION OF PLATFORM PITCH IN THE CASE WITH NO CURRENT

The model over predict the pitch displacement amplitude although the frequency agrees with the experiment. Both surge and pitch motion signals are fluctuated regularly. Regular fluctuation also found in model and experiment signals of platform motions in surge and pitch for the case with applied current. The surge and pitch signals are shown in Figure 9 and 10 respectively.

The platform surge and pitch motion from the model are identical with the experiment. The surge motion from the model has the same amplitude but with different magnitude range. The average displacement from model is slightly higher than the result from the experiment. This condition does not reflect on platform pitch motion as shown in Figure 10.

In the model with applied current, platform pitch motion agrees with experiment with slightly higher amplitude. The orientation discrepancy is likely due to imprecise response amplitude operator estimation between the model and experiment.

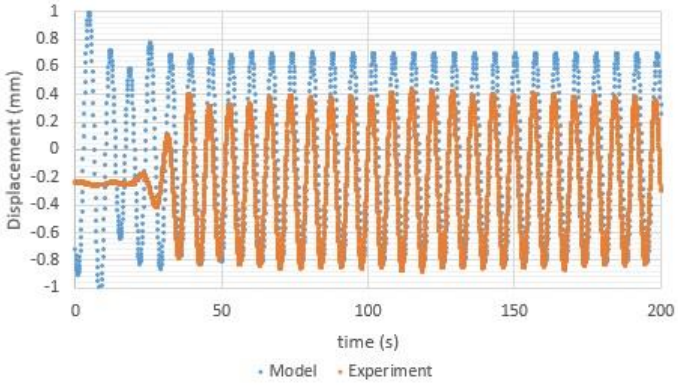

FIGURE 9. VALIDATION OF PLATFORM SURGE IN CASE WITH CURRENT

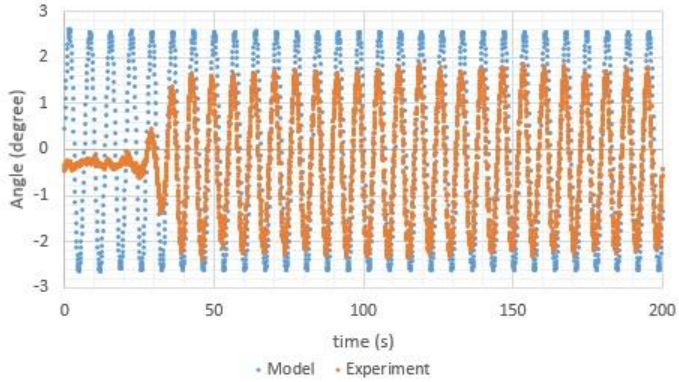

FIGURE 10. VALIDATION OF PLATFORM PITCH IN CASE WITH NO CURRENT

4.2. MOORING PERFORMANCE

The mooring performance analysis evaluates the validated mooring line under horizontal axis (HAT) and vertical axis turbine (VAT) operations. In this mooring performance model, the irregular wave of JONSWAP mode is employed. The model run with environment condition as written in Table 1.

The model utilizes a horizontal turbine from Instream Turbine (SIT) manufactured by SCHOTTEL [11]. The turbine performance has been tested by Starzman et. Al [17, 18] and its thrust property from the test is applied in the model. A turbine thrust performance specifies drag coefficient produced by the sea flow under various turbine's operation. As a tidal turbine operates, seawater velocity is magnified and influence to its drag force. This will affect to fluid loading acting on the mooring lines. The data is employed in OrcaFlex model to obtain mooring life time. The life time is presented in yearly basis along the mooring line length.

The vertical axis tidal turbine from [3] is utilized in the model. [3] conducted experiment of three bladed vertical axis tidal turbine constructed from NACA 0020 blades. From the

experiment turbine thrust from various current speed was found and applied in the model. The VAT and HAT have similar coefficient of performance (Cp) variation working at a certain tip speed ratio (TSR) range. The HAT has Cp of 0.4 working at TSR equals to approximately 4 [17]. The VAT works with maximum Cp of 0.38 at TSR of 3.2 [3].

The turbines are modelled with pipe line structures in which the variable thrust data is linked. The turbines are connected at the bottom of the platform and positioned fully submerged in the seawater. VAT and HAT turbine's specifications are given in Tables 3 and 4 respectively. The turbine model in OrcaFlex is shown in Figure 11.

TABLE 3. VERTICAL TURBINE SPECIFICATION [3]

Rotor diameter (m)	6.45
Height (m)	4.84
Blade root chord (m)	0.4
Blade tp chord (m)	0.24
Blade profle	NACA 0021
pitch	0

TABLE 4: HORIZONTAL TURBINE SPECIFICATION [16]

Rotor diameter (m)	4
Rated electronic power (kW)	62
Rated water velocity (m/s)	3
cut-in speed (m/s)	0.8
cut-out speed (m/s)	6
Nacelle weight (ton)	1

FIGURE 11: MOORING CHAIN TENSION WITH A TURBINE MOUNTED

The mooring performance is evaluated using 24 variations of environment. [19] has identified the british ocean wave velocity which has range from 1 m/s to 4 m/s. The wave velocity in the model is selected from that range accordingly. The wave direction is varied from 0 until 350 degree with 45 degree increment. There are four current speeds used for this model. They are 0.75, 1, 1.25, and 2 m/s.

The mooring chain properties is written in Table 2 and manufactured from steel grade 4 (R4). The fabrication and treatment of standard grade 4 mooring chain is referred to DNV-OS-E302 Offshore Mooring Chain [6]. The T-S for typical mooring chain steel curve has been tested by [7]. The mooring line 1 tension generated under VAT and HAT operation is illustrated in Figure 12

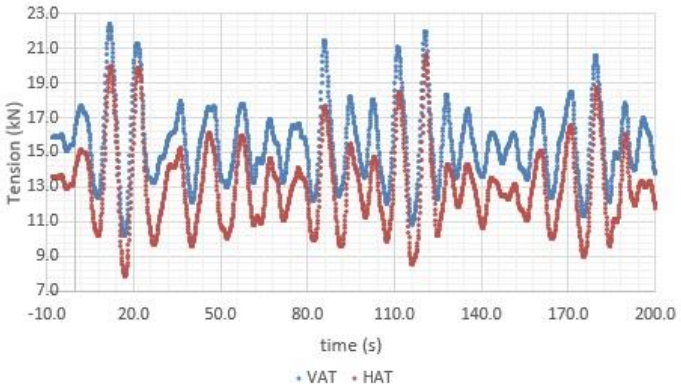

FIGURE 12: MOORING LINE TENSION UNDER TURBINE OPERATION

From Figure 12 it can be seen that mooring line tension under VAT is slightly higher than HAT operation. However the line profile for both turbines operation are identical. The higher tension of VAT operation is due to higher drag force at a certain Reynolds number (Re). The higher drag force indicates higher viscous effect which tends to increase the fluid loading on the mooring line. At lower Re, the selected vertical turbine drag force is increased drastically. This generates higher line 1 tension as shown in Figure 1.

The platform surge and pitch motion under both turbines operation are depicted in Figures 13 and 14 respectively.

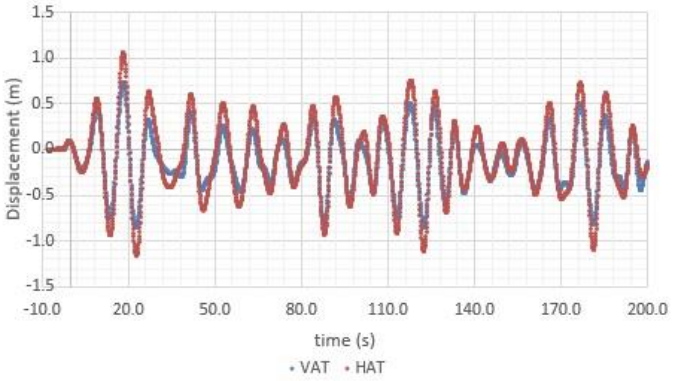

FIGURE 13: PLATFORM SURGE MOTION UNDER TURBINE OPERATION

Figures 13 and 14 show that platform surge and pitch motions under VAT and HAT operations are identical. This is likely due to identical environment condition used for both turbine

operations. The turbines are located under the sea surface thus it does not affect to fluid loading on sea surface hitting the platform. However the platform surge motion under VAT operation in Figure 13 is found slightly lower than HAT. The displacement is influenced by fluid viscous force. Higher viscous force is generated by higher drag force is produced in VAT operation.

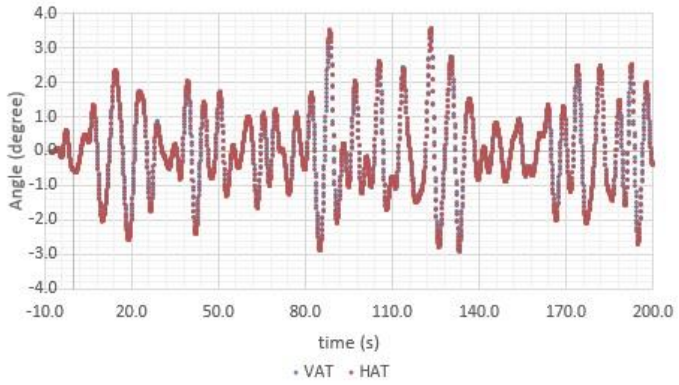

FIGURE 14: PLATFORM PITCH MOTION UNDER TURBINE OPERATION

From Figures 12, 13, and 14, it can be seen that turbines generates dynamic loading which also raises fatigue risk and failure on the mooring line structure. The fatigue analysis determines how a mooring line survives with the dynamic loading for environment and influences its lifetime. The mooring line lifetime under VAT and HAT operation are depicted in Figure 15. The mooring line zero pint is taken at the fairlead point on the platform. The length is measured down from the fairlead to the anchor point. From Figure 8, it can be seen that the mooring line life time is increasing along the mooring line. It increases significantly starting at 20 m length approximately. At this point, the mooring line is in contact with seabed at which the line lies on the seafloor and does not experience small fluid loading. The corrosion and abrasive effects are neglected in this analysis. As approaching the anchor, the line has less motion thus the life time becomes higher. The mooring lifetime for VAT operation is 81.4 years whereas HAT use is 60

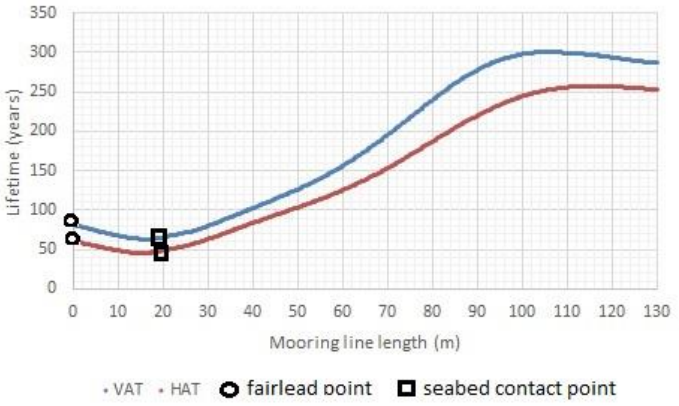

FIGURE 15: MOORING LINE LIFETIME UNDER VAT AND HAT OPERATIONS

The mooring line zero point is taken at the fairlead on the platform. The length is measured down from the fairlead to the anchor. Figure 15 shows that the mooring line lifetime under both turbine operations are increasing from the mooring line zero point. It also increases significantly starting at approximately 20 m length. At this point, the mooring line is in contact with seabed such that the line lies on the seafloor and experience very small fluid loading. The corrosion and abrasive effects are neglected in this analysis. Mooring line lifetime under VAT operation is found higher because of higher tension. Under higher tension condition, a line has less fluctuation as it is more rigid so that the structure becomes more steady. Therefore the structure experience less fatigue failure and has longer lifetime.

5. CONCLUSION

The feasibility of a mooring line for a double hull floating tidal energy platform is investigated in this paper. The investigation is performed by validating the mooring line numerical model against experimental result with 1:12 scale ratio. Tension line, and surge and pitch platform motions are validated to ascertain the validity of the model. Further the result is applied to demonstrate the mooring line performance when a turbine is mounted and operated at a set environmental condition.

The validation process shows that mooring line tension and platform motions from numerical models with current and no applied current agree with the ones from the experiment. The small discrepancies are found in the platform motions but less than 10%. The tension under VAT operation is also found higher however this gives longer mooring line lifetime.

ACKNOWLEDGEMENTS

This research is supported by Innovate UK (IUK103499) for the project of Modular Tidal Generator (MTG) and Offshore Renewable Energy Group, CEMPS, University of Exeter is one of the consortium members.

REFERENCES

[1] Al-Solihat, M.K. and Nahon, M., 2014, September. Mooring and hydrostatic restoring of offshore floating wind turbine platforms. In *Oceans-St. John's, 2014* (pp. 1-5). IEEE.

[2] Azcona, J., Munduate, X., González, L. and Nygaard, T.A., 2017. Experimental validation of a dynamic mooring lines code with tension and motion measurements of a submerged chain. *Ocean Engineering*, *129*, pp.415-427.

[3] Bachant, P., Wosnik, M., Gunawan, B. and Neary, V.S., 2016. Experimental study of a reference model vertical-axis cross-flow turbine. *PloS one*, *11*(9), p.e0163799.

[4] Crudu, L., Obreja, D.C. and Marcu, O., 2016, August. Moored offshore structures-evaluation of forces in elastic mooring lines. In *IOP Conference Series:*

Materials Science and Engineering (Vol. 147, No. 1, p. 012096). IOP Publishing.

[5] DNVGL-RP-C205 Environmental conditions and environmental loads. Accessed on Oct 12, 2018. https://rules.dnvgl.com/docs/pdf/DNVGL/RP/2017-08/DNVGL-RP-C205.pdf

[6] DNV-OS-E302 Offshore Mooring Chain, DNV, October 2013. Accessed on Nov 15, 2018. https://rules.dnvgl.com/docs/pdf/DNV/codes/docs/2013-10/OS-E302.pdf

[7] Fernández, J., Storesund, W. and Navas, J., 2014, June. Fatigue performance of grade r4 and r5 mooring chains in seawater. In *ASME 2014 33rd International Conference on Ocean, Offshore and Arctic Engineering* (pp. V01AT01A035-V01AT01A035). American Society of Mechanical Engineers.

[8] Ghafari, H. and Dardel, M., 2018. Parametric study of catenary mooring system on the dynamic response of the semi-submersible platform. *Ocean Engineering*, *153*, pp.319-332.

[9] Harris, R.E., Johanning, L. and Wolfram, J., 2004. Mooring systems for wave energy converters: A review of design issues and choices. *Marec2004*.

[10] https://www.orcina.com/ Accessed on Dec 19, 2018

[11] https://www.schottel.de/schottel-hydro/sit-instream-turbine/ Accessed on Dec 13, 2018

[12] Martinelli, L., Spiandorello, A., Lamberti, A. and Ruol, P., 2010, October. Dynamic model for catenary mooring: Experimental validation of the wave induced load. In *Comsol Conference*.

[13] N. Xie, E. J. Ramsley, S. Brown, D. Graves., R. Nichols-Lee, L. Johanning, P. Weston, E. Guerrini (2018). Renewable tank experiment of a floating, tidal stream energy device. Advances in Renewable Energies Offshore

[14] Segura, E., Morales, R. and Somolinos, J.A., 2017. Cost assessment methodology and economic viability of tidal energy projects. *Energies*, *10*(11), p.1806.

[15] Senjanović, I., Hadžić, N. and Vladimir, N., 2011. Restoring stiffness in the hydroelastic analysis of marine structures. *Brodogradnja: Teorija i praksa brodogradnje i pomorske tehnike*, *62*(3), pp.265-279.

[16] Senjanović, I., Hadžić, N., Vladimir, N. and Tomić, M., 2013. Restoring stiffness formulations and their influence on ship hydroelastic response. *Developments in Maritime Transportation and Exploitation of Sea Resources/Carlos Guedes Soares & Fernando Lopez Pena (ur.).-London: Taylor & Francis Group, 2013. 381-393 (ISBN: 978-1-138-00124-4).*, pp.381-393.

[17] Starzmann, R., Goebel, I. and Jeffcoate, P., 2018. Field Performance Testing of a Floating Tidal Energy Platform–Part 1: Power Performance. *Proc. AWTEC'18*.

[18] Starzmann, R., Jeffcoate, P., Scholl, S. and Elsaesser, B., 2015. Field testing a full-scale tidal turbine part 1: power performance assessment. In *European Wave and Tidal Energy Conference* (Vol. 2015).

[19] Tidal Power in the UK. Research Report – UK case studies. Sustainable Development Commision, October 2007. http://www.sd-commission.org.uk/data/files/publications/TidalPowerUK5-UK_case_studies.pdf